Theor Chem Acc (2007) 117: 29–39
DOI 10.1007/s00214-006-0125-1

REGULAR ARTICLE

Alexander Schnurpfeil · Martin Albrecht

Charge transport properties of molecular junctions built from Dithiol polyenes

Received: 15 December 2005 / Accepted: 27 January 2006 / Published online: 11 May 2006

Abstract We present a study of the charge transmission behavior of a series of dithiol polyenes in the context of molecular junctions. Using the Landauer theory and zero voltage approximation the Green's functions of the inserted molecules are calculated from a fully ab initio wave function based procedure. Various possibilities in approximating the correlation space are explored and quantitatively evaluated. Our results show that the transmission behavior of a molecular junction is not a monotonic function of the length of the employed molecule. Moreover, we introduce the analytic solution of a suitable model system to countercheck the ab initio results and find a remarkable degree of correspondence.

Keywords Ab initio methods · Electronic correlation · Charge transport

1 Introduction

Recent years have seen a steep rise in the broad field of nano engineering with molecular junctions being a significant part of it [1]. This has been brought about by tremendous advances in engineering techniques, which lead to both unraveled reduction in size and variety [2]. The particular interest in molecular junctions is to ultimately design switches or 'transistors' on a nano scale which might be triggered by various phenomena. The prototype molecular junction consists of two gold electrodes produced in break–junction experiments, which capture an organic molecule in between that can bind covalently to the electrodes via sulfide bridges [3].

A. Schnurpfeil (✉)
Institute for Theoretical Chemistry, University of Cologne,
50939 Köln, Germany
Tel.: +49-221-4706885
E-mail: a.schnurpfeil@uni-koeln.de

M. Albrecht
Theoretical Chemistry FB08, University Siegen, 57068 Siegen,
Germany

The theory of charge transport through molecular junctions is, however, notoriously difficult. Most theoretical descriptions try to illuminate partial aspects like the role of the molecular electronic structure [4–6] or the influence of various structural conformations [7–9]. It is most prominently the set of methods based on the local density approximation (LDA) to density functional theory (DFT) as a starting point, which provides numerically affordable applications to the molecular junction problem [4–10] (cf. Refs. [4–8,10] for applications to carbon wires and benzene–based systems). Further approximations are commonly built on top of LDA, like the tight binding approach (TB) or parametrized minimal basis sets [11]. Another set of approaches renounces completely the attempts of ab initio calculations and resorts to empirical models [12–16]. Most recently the DFT based augmented plane–wave method was applied to monowires by Mokrousov et al. [17]. Examples for further approximations are given by Guitierrez et al. in an application to an all–carbon system with capped nanotubes as electrodes [11], Fagas et al. with an analysis of the off–resonant electron transport in oligomers (G. Fagas, A. kambili and M. Elstner, Submitted) and Cuniberti et al. with an investigation of the role of the contacts [18,19]. An application predicting the actual current-voltage behavior of two aromatic molecules was demonstrated by Heurich et al. [20]. A more advanced scheme developed by Xue, Ratner and Datta sticks with these approximations, but develops a non–equilibrium formalism [13,15, 21,22]. Earlier attempts were presented by Wang, Guo and Taylor. [23–25]. Principle ideas go back to Caroli et al. who originally focused on non–interacting systems [26]. While conceptually somewhat different, for the case of dc currents the ansatz of Cini is known to yield the same results [27]. The steady–state procedures have then been formulated as DFT schemes along the lines proposed by Lang [28]. However, possibly due to inherent shortcomings of the LDA approach, some results are far off experimental data. Calculations of Di Ventra et al. turned out to be off by two orders of magnitude [6,29], while different functionals are found to lead to large fluctuations of one order of magnitude [29,30]. The reason behind this is assumed to be the fact that transmission

functions obtained from static DFT approaches have resonances at the Kohn–Sham eigenenergies, which frequently do not coincide with the physical excitation energies. In contrast, a most recent wave function based ab initio approach based on scattering theory came into the range of experiments for the same kind of organic systems [31].

Wave function based methods, on the other hand, are straightforwardly applicable to both ground state and excited state calculations alike. Subsequently, quantities like the self energy or the transport coefficient T can be obtained in a reliable manner. Furthermore, they are amenable to systematic improvement on the numerical accuracy. However, the numerical demand increases tremendously with the system size. A demonstration of a wave function based calculation of the transport current through a molecular junction was recently given by the aforementioned work of Delaney and Greer [31]. Their original approach was directly derived from scattering theory, thus avoiding the calculation of any Green's function. The general bottle–neck of steep increase of numerical effort with system size, however, affects all wave function based methods alike. It is precisely this obstacle which can be overcome by a formulation of electron correlations in local orbitals and a hierarchy of correlation contributions called the incremental scheme. The usefulness of local orbitals has recently been confirmed in the frame of an LDA tight binding approach to transport properties of nanowires [32–34] as well as carbon nanotubes [35].

One of the authors has developed a wave function based ab initio method to obtain the Green's function of semiconductors [36–39]. The key enabling such calculations for solids was an approach based on local orbitals and a real space formulation of the self energy. In a recent development similar ideas were shown to bring about significant progress for the case of molecules. Applications have been performed for dithiolbenzene and its meta version [40,41]. Furthermore a first attempt to extend this approach to the non–equilibrium case has been made most recently [42,43], albeit in a minimal basis set.

In this paper, we stick to the Landauer approximation applied earlier to dithiolbenzene [40,41]. Our procedure is applied to a series of dithiol polyenes with increasing chain length. The transmission coefficient T is obtained and discussed as a function of the chain length. Various ways of setting up the Green's function and the transmission coefficient are considered. The results are then compared to a model chain.

In Sect. 2 we briefly summarize the theory underlying our formalism. The numerical results obtained for the dithiol polyenes are presented in Sect. 3 and are confronted with the findings of a model system for which analytic formulas are computed in Sect. 4 Our conclusions are given in Sect. 5

2 Theory

2.1 The Green's function

Our correlation scheme is formulated in terms of local occupied and local, or alternatively canonical, virtual HF orbitals. On the basis of these orbitals the one–particle Green's function is set up. As an example we restrict our discussion to the case of virtual molecular states, as the case of occupied states is completely analogous. The model space P describing the HF level then comprises of the $(N+1)$–particle HF determinants $|n\rangle$, while the correlation space Q contains single (and, in principle, double) excitations $|\beta\rangle$ on top of $|n\rangle$:

$$|n\rangle = c_n^\dagger |\Phi_{\mathrm{HF}}\rangle, \qquad |\beta\rangle = c_r^\dagger c_a |n\rangle, \quad c_r^\dagger c_s^\dagger c_a c_b |n\rangle \tag{1}$$

$$P = \sum_n |n\rangle\langle n|, \qquad Q = \sum_\beta |\beta\rangle\langle\beta|. \tag{2}$$

In this local description indices provide an orbital index n which is normally taken to indicate a local HF orbital and includes the spin index. We adopt the convention that indices $a, b, \ldots$ refer to occupied HF orbitals, $r, s, \ldots$ denote virtual orbitals and $m, n, \ldots$ can be either occupied or unoccupied orbitals. The idea of local orbitals given above translates into a restriction of the area the orbital can be chosen from to one or more contiguous spatial parts of the molecule. It is important to note that by enlarging the size of the spatial area thus covered this approximation can be checked in a systematic way for convergence. This leads to the incremental scheme introduced in Sect. 2.3.

Pertaining to the above notation the Green's function matrix $\mathbf{G}$:

$$G_{\mathrm{nm}}(t) = -i\,\langle T[c_{\mathrm{n}}(0) c_{\mathrm{m}}^\dagger(t)]\rangle, \tag{3}$$

where T is the time–ordering operator and the brackets denote the average over the exact ground state, which can be obtained from Dyson's equation as:

$$G_{nm}(\omega) = [\omega \mathbf{1} - \mathbf{F} - \Sigma(\omega)]^{-1}_{\mathrm{nm}}\,. \tag{4}$$

Here the self energy $\Sigma(\omega)$ which contains the correlation effects, has been introduced, $\mathbf{1}$ is the identity matrix and $\mathbf{F}$ the Fock matrix. The correlated eigenenergies are given by the poles of the Green's function which are numerically, iteratively retrieved as the zeros of the denominator in Eq. (4). The density of states and satellites can also be obtained from $\mathbf{G}$. To construct the self energy the resolvent

$$\left[\omega - H^{\mathrm{R}} + i\epsilon\right]^{-1}_{\beta;\beta'} \tag{5}$$

is needed. Here ϵ is an infinitesimal positive number and plays the role of a convergence factor in the standard notation of the Green's function theory which is taken to be zero in the end. The eq.(5) can be gained from diagonalization of the Hamiltonian matrix

$$[H^{\mathrm{R}}]_{\beta,\beta'} := \langle\beta|H - E_0|\beta'\rangle, \tag{6}$$

where the states $|\beta\rangle$, $|\beta'\rangle$ are those of the correlation space Q as in Eq. (1). The superscript 'R' serves as a reminder that stick to the description of the case of a model space P of all $(N+1)$–particle states and its respective correlation space Q, which is linked to the retarded part of the Green's function. The analogous formulas for the $(N-1)$–particle case would carry a superscript 'A', as this space is linked to the

advanced part. H represents the full standard non–relativistic Hamiltonian operator of the system under consideration and E_0 is its HF ground state energy. Explicit expressions for the matrix elements (6) are given in Eq. (11) of Ref. [37] and go back to an ansatz of Takahashi and Igarashi [44].

A decisive boost in numerical efficiency was brought about by combining the method described with the aforementioned incremental scheme formulated in local HF orbitals [36,37,45,46].

At this point we briefly introduce the notion of a molecular junction. Figure 1 visualizes the concept. A molecule (such as a dithiol polyene) is fixed between two gold electrodes. The sulfur of the thiol groups has a high affinity to gold and will build a covalent type of bonding to the electrodes. The molecule can thus be regarded as a conductor (junction) conducting the current from one electrode to the other.

2.2 The Landauer theory

From the Green's function, the transport coefficient T can be straightforwardly obtained in the frame of the Landauer formalism [47]. This theory constitutes an approximation, assuming zero voltage across the junction, which is frequently adopted and finds its justification in the zero-current theorem [14].

In this context T is given by

$$T = \mathrm{Tr}\,\{\Gamma_\mathrm{L}\,\mathbf{G}\,\Gamma_\mathrm{R}\,\mathbf{G}^\dagger\}, \tag{7}$$

$$\Gamma_\alpha = i[\Sigma_\alpha - \Sigma_\alpha^\dagger], \tag{8}$$

$$\Sigma_\alpha = \mathbf{H}_{\mathrm{M}\alpha}\mathbf{G}^0_{\alpha\alpha}\mathbf{H}_{\alpha\mathrm{M}}, \tag{9}$$

$$\alpha = \mathrm{L}, \mathrm{R}, \tag{10}$$

where the indices 'L' and 'R' refer to the regions on the left ('L') and on the right ('R') of the central region of the molecular junction. The latter is denoted by a subscript 'M' in the above equations and might consist either of the molecule in the junction alone or could also include adjacent parts of the electrodes. At this general level, this remains unspecified. The notation used in this section refers to a standard partitioning theory, where a system comprising of regions L, M and R is folded onto an effective system which is only described by region M, but which incorporates the effects of the regions L and R.

The coupling to the left (L) and the right (R) electrode can be obtained from the self energies of the respective coupling regions as shown in Eq. (8). The self energies in turn are obtained in this partitioning approach as depicted in Eq. (9). This equation requires, in principle, the exact knowledge of the isolated lead surface Green's function $\mathbf{G}^0_{\alpha\alpha}$ for both sides of the junction ($\alpha = \mathrm{L}, \mathrm{R}$). In the wide band approximation, which has been adopted throughout this work, the coupling self energies provide an overall widening of the molecular energy levels, in particular at the sulfide bridges, due to the interaction with the energy continuum provided by the metal [5]. This approximation introduces a coupling between molecule and electrodes parametrized by a coupling constant δ which replaces the evaluation of Eq. (9). However, the bare Green's function for the central region, $\mathbf{G}^0_{\mathrm{MM}}$, is obtained in a fully ab initio manner from the Green's function theory put forth in the previous section. The superscript '0' indicates that the bare Green's function of the central region is calculated, with the effect of the electrodes being ignored, hence the notion 'bare'.

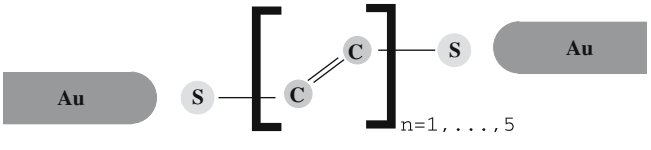

Fig. 1 Illustration of a molecular bridge. The molecule is coupled to the gold electrodes via its sulfur atoms. The hydrogens have been suppressed in the figure

The Green's function matrix $\mathbf{G}$, on the other hand, represents the entire system including the effects of the electrodes, and is also to be obtained from the partitioning approach leading to:

$$\mathbf{G}_{\mathrm{MM}} = \left[{\mathbf{G}^0_{\mathrm{MM}}}^{-1} - \Sigma_\mathrm{L} - \Sigma_\mathrm{R}\right]^{-1}, \tag{11}$$

For the sake of an efficient evaluation of the key quantity $\mathbf{G}^0_{\mathrm{MM}}$, we employ an incremental scheme to be discussed below in Sect. 2.3. (The scheme is displayed for the key quantity T, but has been shown in earlier applications to also hold for the self energy Σ, hence for the Green's function itself. Details can be found in Refs. [36,37,45]).

2.3 The incremental scheme

As we demonstrated in earlier applications [40,41], the Green's function and hence the transmission coefficient T can be obtained in a step–wise manner by applying the so called incremental scheme.

As an illustration of the incremental scheme, we choose trans–1,2–dithiolbutadiene which is depicted in Fig. 2. As subsets of the system some arbitrary spatial parts of the molecule, representing a suitable partitioning, are chosen. In the figure, the thiol groups are summarized as regions I and IV, respectively, while regions II and III comprise of a $H - C = C - H$ group each. An incremental description of the transmission coefficient T could start with a correlation calculation, in which only excitations inside one of the regions I–VI, e.g. region I, are allowed. This results in a contribution the correlation correction to the self energy, and ultimately to the transmission coefficient T, which is labeled by the region it refers to, e.g. T^I, and constitutes a one–region increment ΔT^I:

$$\Delta T^\mathrm{I} := T^\mathrm{I}. \tag{12}$$

The sum of all one–region increments yields the so called one–region increment approximation (denoted S) to the transmission coefficient. In the next step the calculation is repeated

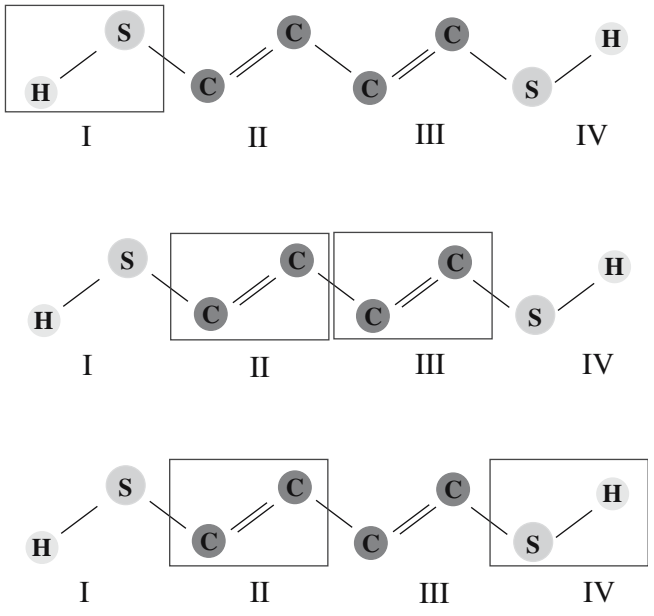

Fig. 2 Sketch of the incremental scheme, exemplifying a possible partitioning of trans–1,4–dithiolbutadiene in four regions. The upper picture denotes a one–region increment (S) in which region I is emphasized by a *box*, the second panel shows a next–neighbor–two–region increment (nD) comprising of regions II and III and the lower picture represents an increment in which region II and region IV are contained to form a next–next–neighbor–two–region increment (nnD). The labeling of other increments is analogous as introduced in Sect. 2.3

with excitations correlating the charge carriers being allowed inside two regions e.g. region II and region III as shown in the middle of Fig. 2. The difference of this extended calculation $T^{\mathrm{II,III}}$ with respect to the one–region increments ΔT^{II} and ΔT^{III} then isolates the effect of additional excitations involving the extended region consisting of region II and region III and forms a two–region increment $\Delta T^{\mathrm{II,III}}$:

$$\Delta T^{\mathrm{II,III}} := T^{\mathrm{II,III}} - \Delta T^{\mathrm{II}} - \Delta T^{\mathrm{III}}. \tag{13}$$

In general, two–region increments are symbolized by D. In particular, this increment will be denoted as next–neighbor–two–region increment (nD). If the two regions involved are second or third next nearest neighbors, the respective increment is denoted by nnD or $nnnD$, respectively.

This procedure can be continued to more and more regions and the naming of this increments is analogous. Equation (14) for example depicts a three–region increment, which will be denoted as T throughout the remainder of this work, whereas M represents results where the entire molecule is included in one increment.

$$\begin{aligned}\Delta T^{\mathrm{I,II,IV}} = {} & T^{\mathrm{I,II,IV}} - \Delta T^{\mathrm{I,II}} - \Delta T^{\mathrm{I,IV}} - \\ & \Delta T^{\mathrm{II,IV}} - \Delta T^{\mathrm{I}} - \Delta T^{\mathrm{II}} - \Delta T^{\mathrm{IV}}\end{aligned} \tag{14}$$

In the end the summation of all increments as in Eq. (15) is the final approximation to the sought transmission coefficient, i.e.:

$$\begin{aligned}T = {} & \textstyle\sum_{\mathrm{A=I}}^{\mathrm{IV}} \Delta T^{\mathrm{A}} + \\ & \textstyle\sum_{\mathrm{A>B=}I}^{\mathrm{IV}} \Delta T^{\mathrm{A,B}} + \\ & \textstyle\sum_{\mathrm{A>B>}C=I}^{\mathrm{IV}} \Delta T^{\mathrm{A,B,C}} + \\ & \ldots\end{aligned} \quad . \tag{15}$$

From the experience gained with the incremental scheme in its application to the self energy, a rapid decrease of increments both with the distance between the regions involved and with their number included in the increment can be expected. This means that only a few increments might need to be calculated. It is crucial to emphasize that the cutoff thus introduced in the summation in Eq. (15) is well controlled, since the decrease of the incremental series can be explicitly monitored. The validity of this point is demonstrated in the discussion of the results. There we will also see that the convergence behavior of the transmission coefficient is even better than the convergence behavior of the correlation correction to excitation energies.

3 Results and Discussion

We start our discussion of the results with the obtained correlation corrected HOMO-LUMO gap of the dithiol polyene oligomers, which we refer to as chains henceforth. In order to shorten the notation, we introduce the abbreviation $\gamma = (\mathrm{LUMO\text{-}HOMO})_{\mathrm{HF}} - (\mathrm{LUMO\text{-}HOMO})_{\mathrm{CORR}}$, where $(\mathrm{LUMO\text{-}HOMO})_{HF}$ denotes the HOMO-LUMO gap on the HF level and $(\mathrm{LUMO\text{-}HOMO})_{\mathrm{CORR}}$ donates the correlated gap. The geometrical structure of the dithiol polyene chains was optimized on the B3LYP–level of DFT with a 6-31G(d) basis set using the quantum chemistry program GAUSSIAN03 [48]. The results of γ are given in Table 1. We started the series of oligomers with trans-1, 2-dithiolethylene and increased the chain length step by step with H–C=C–H fragments. The number of such fragments will be denoted by n. In order to avoid a lengthy notation we abbreviate the molecules by their number of H–C=C–H fragments. For instance, 1, 2-dithiolethylene will be referred to as molecule 1. The first column denotes the molecule under consideration, the second column shows the increments which were used in the calculations in order to get the correlation energies. The calculations were performed in two different ways: the third column in Table 1 represents the results when the entire canonical virtual space, henceforth denoted as space 1, was included in the perturbation calculation. The fourth column contains the results when the virtual space, was localized by the method of Pipek and Mezey [49], henceforth denoted as space 2,using the quantum chemistry package MOLPRO [50]. In both cases, canonical virtual space and localized virtual space,the occupied orbitals were localized by the same method. In the case of space 1 the whole virtual space is assigned to each

increment, while in the case of space 2 only those localized virtual orbitals are included which lie in the particular region of the increment under consideration. For the calculation of the γ's and T's a $cc-pVDZ$ basis set was used. The difference of the numerical effort which results in using space 1 and space 2, respectively, in the calculations is remarkable. While the entire virtual space is included with each increment by using space 1, the virtual space is increased step by step with the use of more and more increments using space 2 until the total virtual space is switched on if the entire molecule is considered as one increment. So it is obvious that the correlation contribution one obtains, e.g. with a one–region increment, is closer to a complete calculation when space 1 instead of space 2 is applied because the correlation space is much larger in the former case. The influence of different correlation spaces can be realized by considering the amount of γ when the entire molecule is included in the calculation. For molecule 1, we obtain 1.839 eV when the virtual space is localized in contrast to 3.032 eV when using the canonical virtual space. This error consecutively becomes smaller and smaller as the chain becomes larger. The difference between these two values amounts to 1.193 eV for molecule 1 and decreases monotonously to 0.566 eV for molecule 5. This is an obvious manifestation of the transition from an oligomer to a polymer: as the oligomer increases in length, including the full virtual space loses, some of its advantage as more and more long distance excitations are accounted for which they do not contribute to the correlation corrections. An obvious manifestation of the oligomer–polymer transition is the decrease of the gap with increasing chain length.

We now focus on the application of the incremental scheme. When space 1 is used the table suggests that the main part of γ can be obtained by computing only the one–region increments S. The difference between γ obtained by considering the entire molecule 1 compared to γ obtained by using the S-increments amounts to merely 0.132 eV. In the case of molecule 2 this difference becomes 0.453 eV. For the remaining molecules the deviations stay in the same range, e. g. 0.424 eV for molecule 5. By contrast, when considering the results computed by using space 2 it is not possible to obtain the main part of γ by only computing the S-increments. For example, the difference in the values for molecule 2 amounts to 1.288 eV, which is significant. It can thus be concluded that it is necessary to use space 1 in order to get reliable results concerning γ while applying a strict cut in the incremental scheme. So we continue our discussion about the incremental scheme by only considering the results obtained with space 1. As mentioned before, it is possible to obtain the main part of γ if the S-increments are alone computed. To go a step further one can include a different number of two–region increments D to improve the results. The more the increments are included the more accurate the result will be. However, a close look at the values in Table. 1 allows to establish that it is sufficient to include only the S- and D-increments in order to get satisfying results. In some cases γ will be a little bit overestimated. This is an effect which is inherent to the incremental scheme. By including more and more increments this effect will be compensated. It is an important feature of this approach that reliable results can be obtained although the incremental scheme will be truncated. This is a decisive factor which allows to avoid the otherwise formidable computational costs inherent to an ab initio treatment. The calculation of γ serves as a check for the incremental scheme which we predominantly used for the calculation of the transmission coefficient. Similar trends in the converging behavior are observed for the transmission coefficient T. Figure 3 shows the devolution of the transmission coefficient with increasing coupling constant δ for molecule 4. When no coupling is assumed the transmission coefficient is zero which is in accordance with the physical intuition. The larger the coupling constant, the larger is the transmission coefficient which has its maximum when a coupling constant of 13 eV is applied. After this point the transmission coefficient is decreasing and tends to zero when a coupling constant of 27 eV is assumed. This behavior can be explained as follows: with an increase in the coupling the density of states (DOS) will also leak into the HOMO-LUMO gap of the bare molecule. This is demonstrated in the case of a rather week coupling of 3 eV in Fig. 4, where the various energy levels of the bare molecule are still discernable, but are clearly broadened somewhat from their otherwise perfect δ–peak shape due to the coupling constant. At the same time, some density of states becomes available in the HOMO–LUMO gap. So the probability of an electron transmission from the valence state to the unoccupied state will also be increased which results in a higher transmission coefficient. Upon excessive increase of this broadening, density will then be transferred into the regions far away from the gap, so that the charge density will be depleted again in the energy region of the original HOMO–LUMO gap and hence the transmission coefficient decreases as well. The most remarkable fact is the fast convergence of the transmission coefficient when the incremental scheme is used. Figure 3 displays the results if different kinds of increments are used for the computation: the solid line represents the transmission coefficient T in dependence of the coupling constant δ for the case that the entire molecule has been correlated. If T is approximated by the one–region increments S, the error resulting from this restriction on the incremental scheme will lead to just a slight overestimation given in percent by the dashed line. On average, the error is just 1% with a peak of 6%. Upon inclusion of the two–region increments D this error is reduced basically to zero as can be seen by the dotted line in the figure. In conclusion this means that it is sufficient to only compute the one–region increments in order to get reliable results for the transmission coefficient. The convergence properties are even better compared to the convergence properties of γ. This finding allows to save considerable numerical cost. Thus, we are lead to believe that in the future it is feasible to perform calculations on significantly larger systems.

In Fig. 5 the transmission coefficients with varying coupling constants are depicted from molecule 1 to molecule 5 for the sake of comparison. For this calculation space 1 was used. As expected, molecule 1 has the highest

Table 1 Correlation correction γ to the HOMO-LUMO gap of the dithiol polyene chains

No of $H-C=C-H$-fragments	Increments	γ using space 1	γ using space 2
1	S	2.900	1.215
	$S+nD$	3.039	1.815
	M	3.032	1.839
2	S	2.373	0.757
	$S+nD$	2.686	1.779
	$S+nD+nnD$	2.810	1.858
	$S+D$	2.827	1.866
	$S+D+nT$	2.827	2.022
	$S+D+T$	2.827	2.041
	M	2.826	2.045
3	S	2.206	0.602
	$S+nD$	2.447	1.575
	$S+nD+nnD$	2.583	1.699
	$S+nD+nnD+nnnD$	2.618	1.721
	$S+D$	2.622	1.724
	$S+D+nT$	2.626	1.902
	$S+D+T$	2.634	1.945
	M	2.639	1.972
4	S	2.104	0.519
	$S+nD$	2.298	1.449
	$S+nD+nnD$	2.440	1.600
	$S+nD+nnD+nnnD$	2.481	1.637
	$S+nD+nnD+nnnD+nnnnD$	2.491	1.644
	$S+D$	2.492	1.645
	M	2.521	1.923
5	S	2.021	0.405
	$S+nD$	2.179	1.317
	$S+nD+nnD$	2.334	1.484
	$S+nD+nnD+nnnD$	2.380	1.533
	M	2.445	1.878

The obtained values using space 1 and space 2 are given in columns three and four, respectively. The employed increments are indicated in the second column. The computed dithiol polyenes are designated by the number n of their $H-C=C-H-$fragments according to Fig. 1. The notation S, nD, etc. is as introduced in Sect. 2.3. Values are in eV

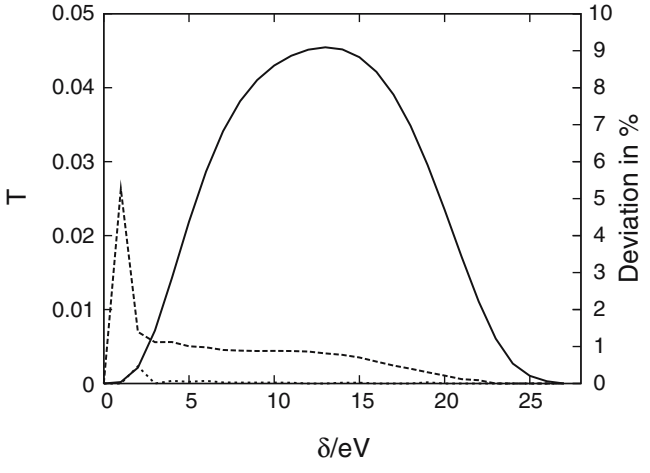

Fig. 3 The transmission coefficient T with varying values of the coupling constant δ for molecule 4 is depicted by the *solid line*. The entire molecule is used as one increment M. The *dashed line* shows the overestimation of T in percent if only all single increments S are included in the calculation. The *dotted line* depicts this overshooting of T if all S and double increments D are included in the calculation

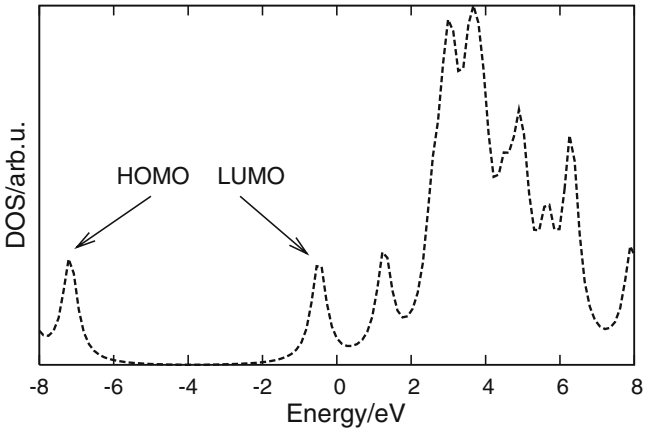

Fig. 4 Correlation corrected DOS of molecule 4 for a coupling constant δ of 3 eV

transmission coefficient T compared to the other dithiol polyenes under consideration. The maximum for this molecule occurs at a coupling constant of 11 eV. The same coupling constant gives the biggest value of the transmission coefficient of molecule 2 which has the second highest transmission coefficient T, as expected. However, as we continue beyond molecule 3, the transmission coefficient increases again, contrary to intuition, and the maximum value is shifted to a higher value of the coupling constant, specifically 18 eV. Intuition might suggest that the conduction properties of *molecule 3* are

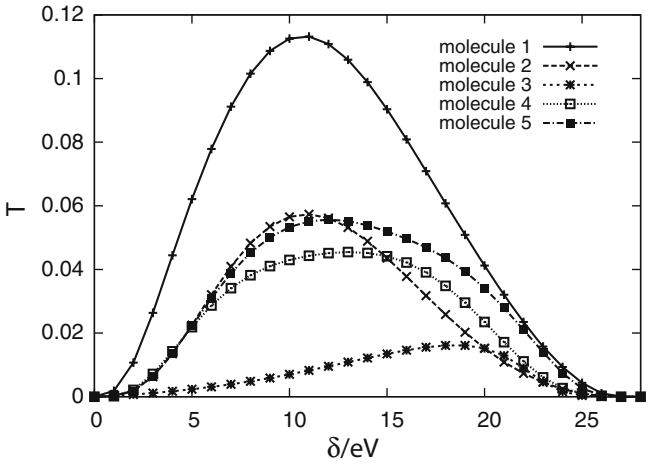

Fig. 5 The transmission coefficient with varying values of the coupling constant δ from molecule 1 to molecule 5

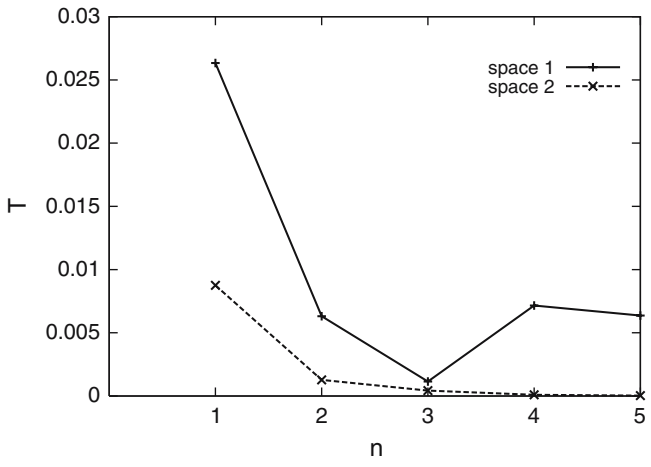

Fig. 6 Results of the transmission coefficients from molecule 1 ($n = 1$) to molecule 5 ($n = 5$) using space 1 and space 2, respectively. The coupling constant δ is set to 3 eV

somewhat better compared to molecule 4 and *molecule 5* but the reverse is found. The maxima of the transmission coefficients of molecule 4 and molecule 5 lie above the values ofmolecule 3 in the same range of the coupling constant of molecule 1 and molecule 2. In order to explain this anomalous behavior the following aspects are of importance. Firstly, the size and hence the length of the molecule plays a decisive role. The smaller the molecule between the electrodes the higher tunneling–like effects across the molecule might be. This helps to understand the relatively high conduction characteristics of molecule 1 and molecule 2 and the reduced conduction qualities of molecule 3. A second aspect is the conjugation of the π-system of these molecules. As the chain length increases, the π–system gets ever more delocalized, thus facilitating conduction.

Finally, the situation in energy space is also of interest. With increasing size of the molecule the HOMO–LUMO gap decreases, thus again facilitating charge transport. To some extent this last point is a rephrasing of the second, as it is the delocalization of the π–system which leads to a gap reduction with the chain length.

In this respect it is instructive to look at molecule 4 and molecule 5. Here we observe an increase of the transmission coefficient compared to molecule 3. This results presumably from the increasing conjugation effect of the π–systems. Since the highest value of the transmission coefficient of molecule 5 is even higher than the highest value of the transmission coefficient of molecule 4, one can assume that the conjugation effect overcompensates the decreasing conducting effects which follow from the increase of the system dimensions.

We proceed our discussion by considering the computed transmission coefficients of the dithiol polyenes using space 1 and space 2, respectively. The results are given in Fig. 6. A coupling constant of 3 eV is assumed. Concerning space 1, the upper curve in Fig. 6 serves as a vertical cut of the diagrams in Fig. 5 at $\delta = 3$ eV. The lower curve in Fig. 6 shows the transmission coefficients when space 2 is used rather than space 1 in the calculations. The values are smaller because the correlation space is too small in order to assess all significant contributions to the transmission as discussed above. This behavior suggests that inclusion of the full canonical virtual space in the calculation is advisable so as to get converged results. We take this as a strong indication for the importance of the conjugated π–system, which is only evidently accounted for if the full virtual space is included.

At present, we were not able to go to longer chains due to the increase in numerical cost. To further illuminate the above findings, we therefore introduce a simple model which allows for analytic solutions for any chain–length in the following section.

4 Model calculations

In order to countercheck the quantum chemical results of the previous section we have set up an exactly solvable model system. It contains $n =: \eta - 2$ identical units $U_i, i \in \{2, 3, \cdots, \eta - 1\}$, each of which contributes a virtual orbital d with energy ϵ_d. The units are thought of to be arranged in the way of a one–dimensional chain. In addition, at the left and right end we add another such unit with indices 1 and η, respectively. These are, contrary to the rest, coupled to electrodes and thus acquire the function of the sulfur bridges of the polyenes of the previous section, while the n units in between serve to mimic the $(CH)_2$ units of the polyenes. As in the previous sections the coupling is taken into account in the frame of the wide band approximation, so that the energy levels of these two units are broadened by an amount δ, which is the external coupling constant.

We then apply a tight–binding scheme so that each unit only interacts with its two neighbors with an interaction strength t.

4.1 The bare chain model

First,the problem of a bare chain without contacts to a reservoir is considered. The Green's function

$$\mathbf{G}(\omega) = \begin{pmatrix} g_{11} & g_{12} & \cdots & g_{1\eta} \\ g_{21} & g_{22} & \cdots & g_{2\eta} \\ \vdots & & & \\ g_{\eta 1} & g_{\eta 2} & \cdots & g_{\eta\eta} \end{pmatrix} \tag{16}$$

describing this system must then fulfill the equation:

$$\begin{pmatrix} g_{11} & g_{12} & \cdots & g_{1\eta} \\ g_{21} & g_{22} & \cdots & g_{2\eta} \\ \vdots & & & \\ g_{\eta 1} & g_{\eta 2} & \cdots & g_{\eta\eta} \end{pmatrix} (-t) \begin{pmatrix} \frac{\omega-\epsilon_d}{-t} & 1 & 0 & 0 & \cdots & 0 \\ 1 & \frac{\omega-\epsilon_d}{-t} & 1 & 0 & \cdots & 0 \\ 0 & 1 & \frac{\omega-\epsilon_d}{-t} & 1 & \cdots & 0 \\ \vdots & & & & & \\ 0 & 0 & 0 & \cdots & 1 & \frac{\omega-\epsilon_d}{-t} \end{pmatrix}$$
$$= \begin{pmatrix} 1 & 0 & 0 & \cdots & 0 \\ 0 & 1 & 0 & \cdots & 0 \\ \vdots & & & & \\ 0 & 0 & 0 & \cdots & 1 \end{pmatrix}. \tag{17}$$

In the following we subsume the parameter t into the Green's function ($g_{ij} \to -t g_{ij}$) and use the abbreviation $\Omega := \frac{\omega-\epsilon_d}{-t}$. Writing out this matrix equation just for the elements of the first line of the Green's function then yields the system of equations:

$$g_{11}\Omega + g_{12} = 1 \tag{18}$$
$$g_{11} + g_{12}\Omega + g_{13} = 0 \tag{19}$$
$$g_{12} + g_{13}\Omega + g_{14} = 0 \tag{20}$$
$$\vdots$$
$$g_{1,\eta-1} + g_{1,\eta}\Omega = 0,$$

which can be rewritten as

$$g_{10} + g_{11}\Omega + g_{12} = 0 \tag{21}$$
$$g_{11} + g_{12}\Omega + g_{13} = 0 \tag{22}$$
$$g_{12} + g_{13}\Omega + g_{14} = 0 \tag{23}$$
$$\vdots$$
$$g_{1,\eta-1} + g_{1,\eta}\Omega + g_{1,\eta+1} = 0, \tag{24}$$

with the agreement

$$g_{10} := -1 \tag{25}$$
$$g_{1,\eta+1} := 0, \tag{26}$$

so that all equations have the form:

$$g_{1,j-1} + g_{1,j}\Omega + g_{1,j+1} = 0, \qquad j \in \{1, 2, \ldots, \eta\}. \tag{27}$$

This leads to the iteration scheme

$$g_{1,j+1} = -g_{1,j}\Omega - g_{1,j-1}. \tag{28}$$

In particular, we have

$$g_{1,\eta+1} = -\Omega g_{1,\eta} - g_{1,\eta-1}. \tag{29}$$

Replacing $g_{1,\eta}$ with the recursion (28) results in

$$g_{1,\eta+1} = \left(\Omega^2 - 1\right) g_{1,\eta-1} + \Omega g_{1,\eta-2}. \tag{30}$$

Continued iteration yields

$$g_{1,\eta+1} = -\Omega\left(\Omega^2 - 2\right) g_{1,\eta-2} - \left(\Omega^2 - 1\right) g_{1,\eta-3} \tag{31}$$
$$= \left(\Omega^4 - 3\Omega^2 + 1\right) g_{1,\eta-3} + \Omega\left(\Omega^2 - 2\right) g_{1,\eta-4}. \tag{32}$$

In general, we find

$$g_{1,\eta+1} = \kappa_j g_{1,\eta-j} - \kappa_{j-1} g_{1,\eta-j-1}, \tag{33}$$

where we have introduced the κ–polynomials

$$\kappa_j := (-1)^{j+1} \Bigg[\Omega^{j+1} - j\Omega^{j-1} + (j-2)\Omega^{j-3} - (j-4)\Omega^{j-5} \cdots \begin{cases} (-1)^{\frac{j}{2}} 2\Omega & j \text{ even} \\ \text{for} & \\ (-1)^{\frac{j+1}{2}} & j \text{ odd} \end{cases} \Bigg]$$
$$= (-1)^{j+1} \left[\Omega^{j+1} + \sum_{l=1}^{L} (-1)^l (j-2l+2) \Omega^{j-2l+1} \right], \tag{34}$$
$$j+1 =: 2L + r, \qquad r \in [0, 1]$$
$$\Leftrightarrow L = \frac{(j+1) - \mathrm{mod}(j+1, 2)}{2}.$$

Here $j+1$ has been expressed in terms of multiples L of 2 plus a remainder r by means of the conventional function $\mathrm{mod}(m, n)$.

Choosing $j = \eta - 1$ in Eq. (33) yields

$$g_{1,\eta+1} = \kappa_{\eta-1} g_{1,1} - \kappa_{\eta-2} g_{1,0}, \tag{35}$$

and upon inserting Eqs. (25, 26) this is solved as

$$g_{1,1} = -\frac{\kappa_{\eta-2}}{\kappa_{\eta-1}}. \tag{36}$$

Going backwards in the system of coupled equations (28) yields for the remaining elements of the first line of the Green's function matrix $g_{1,m}$:

$$g_{1,2} = -\Omega\frac{\kappa_{\eta-2}}{\kappa_{\eta-1}} + 1, \tag{37}$$

$$g_{1,m} = \kappa_{m-2}\frac{-\kappa_{\eta-2}}{\kappa_{\eta-1}} + \kappa_{m-3}. \tag{38}$$

The remaining elements of the Green's function can be obtained in an analogous fashion. For the second line the system of Eqs. (21–24) takes a similar form:

$$g_{21}\Omega + g_{22} = 0 \tag{39}$$
$$g_{21} + g_{22}\Omega + g_{23} = 1 \tag{40}$$
$$g_{22} + g_{23}\Omega + g_{24} = 0 \tag{41}$$
$$\vdots$$
$$g_{2,\eta-1} + g_{2,\eta}\Omega + g_{2,\eta+1} = 0. \tag{42}$$

Again the agreement

$$g_{2,\eta+1} := 0 \tag{43}$$

was used. To obtain the same structure as for the previous case $g_{1,\mathrm{m}}$ the second line Eq. (40) is rewritten as:

$$\tilde{g}_{21} + g_{22}\Omega + g_{23} = 0 \tag{44}$$

$$\tilde{g}_{21} := g_{21} - 1, \tag{45}$$

which in turn allows to rewrite Eq. (39) as:

$$\tilde{g}_{20} + \tilde{g}_{21}\Omega + g_{22} = 0, \tag{46}$$

$$\tilde{g}_{20} := \Omega = -\kappa_0. \tag{47}$$

The system of Eqs. (39–42) can now be solved in the same way as was done above for the system in Eqs. (21–24). The analysis can be continued in the same fashion for all lines j with elements $g_{j,m}$ of the Green's function.

The solutions are found to be:

$$\tilde{g}_{j,m} = \kappa_{j-2} g_{1,m} \tag{48}$$

$$g_{j,m} = \tilde{g}_{j,m}, \qquad m \geq j$$

$$g_{j,m} = \tilde{g}_{j,m} + \kappa_{j-m-2}, \qquad m \leq j.$$

With the convenient definition

$$\kappa_k := 0\,, \qquad k \leq -2 \tag{49}$$

the general solution is finally given by:

$$g_{j,m} = \kappa_{j-2}\left[\kappa_{m-2}\frac{-\kappa_{\eta-2}}{\kappa_{\eta-1}} + \kappa_{m-3}\right] + \kappa_{j-m-2}. \tag{50}$$

As an illustration the problem for $\eta = 3$ is considered. With the solution (50) and the explicit form of the κ–polynomials [Eqs. (34) and (49)] the problem (17) takes the form:

$$\frac{1}{\Omega^2 - 2}\begin{pmatrix} \frac{\Omega^2-1}{\Omega} & -1 & \frac{1}{\Omega} \\ -1 & \Omega & -1 \\ \frac{1}{\Omega} & -1 & \frac{\Omega^2-1}{\Omega} \end{pmatrix}\begin{pmatrix} \Omega & 1 & 0 \\ 1 & \Omega & 1 \\ 0 & 1 & \Omega \end{pmatrix} = \begin{pmatrix} 1 & 0 & 0 \\ 0 & 1 & 0 \\ 0 & 0 & 1 \end{pmatrix}\surd, \tag{51}$$

which indeed works out to be correct.

$$\mid g_{1,\eta} \mid^2 = t^2 \frac{\left[(\kappa_{\eta-3}\Theta + \kappa_{\eta-4} + \delta\Gamma\kappa_{\eta-4})\Omega + \delta(\Gamma\kappa_{\eta-3} - \delta\Theta)\kappa_{\eta-4}\right]^2}{(\Omega^2 + \delta^2)^2}, \tag{62}$$

$$\Theta = -\frac{\delta^2(\kappa_{\eta-4} + \kappa_{\eta-2})(\kappa_{\eta-1} + \kappa_{\eta-3} - \Omega\kappa_{\eta-2}) - \Omega\kappa_{\eta-2}(\delta^2\kappa_{\eta-4} - \delta\kappa_{\eta-2} + \Omega\kappa_{\eta-1})}{\delta^2(\kappa_{\eta-1} + \kappa_{\eta-3} - \Omega\kappa_{\eta-2})^2 + (\delta^2\kappa_{\eta-4} - \delta\kappa_{\eta-2} + \Omega\kappa_{\eta-1})^2},$$

$$\Gamma = \frac{\Omega\delta\kappa_{\eta-2}(\kappa_{\eta-1} + \kappa_{\eta-3} - \Omega\kappa_{\eta-2}) - \delta(\kappa_{\eta-4} + \kappa_{\eta-2})(\delta^2\kappa_{\eta-4} - \delta\kappa_{\eta-2} + \Omega\kappa_{\eta-1})}{\delta^2(\kappa_{\eta-1} + \kappa_{\eta-3} - \Omega\kappa_{\eta-2})^2 + (\delta^2\kappa_{\eta-4} - \delta\kappa_{\eta-2} + \Omega\kappa_{\eta-1})^2}.$$

4.2 The connection to the electrodes

Once the presence of the electrodes is taken into account in the frame of the wide band approximation and the Landauer theory, a slight change to the previous equations has to be added. In fact the Hamiltonian underlying the system changes as:

$$\mathbf{H} := \begin{pmatrix} \Omega & 1 & 0 & \cdots & 0 \\ 1 & \Omega & 1 & \cdots & 0 \\ \vdots & & & & \\ \cdots & 0 & 0 & 1 & \Omega \end{pmatrix} \rightarrow \tilde{\mathbf{H}} := \begin{pmatrix} \tilde{\Omega} & 1 & 0 & \cdots & 0 \\ 1 & \Omega & 1 & \cdots & 0 \\ \vdots & & & & \\ \cdots & 0 & 0 & 1 & \tilde{\Omega} \end{pmatrix}, \tag{52}$$

where we used the abbreviation

$$\tilde{\Omega} := \Omega + i\frac{\delta}{-t}, \tag{53}$$

where δ is again the external coupling constant. The Green's function can still be found by the same procedure as in the previous section. We here give the final solution:

$$g_{j,m} = \kappa_{j-2} g_{1,m} + \kappa_{\mathrm{j-m-2}} \tag{54}$$

$$g_{1,1} = -\frac{\hat{\kappa}_{\eta-2}}{\bar{\bar{\kappa}}_{\eta-1}} \tag{55}$$

$$g_{1,m} = -\frac{\hat{\kappa}_{\eta-2}}{\bar{\bar{\kappa}}_{\eta-1}}\bar{\kappa}_{m-2} + \kappa_{m-3}, \qquad 2 \leq m \leq \eta - 1 \tag{56}$$

$$g_{1,\eta} = -\frac{1}{\tilde{\Omega}}\left(-\frac{\hat{\kappa}_{\eta-2}}{\bar{\bar{\kappa}}_{\eta-1}}\bar{\kappa}_{\eta-3} + \kappa_{\eta-4}\right), \tag{57}$$

where the following shortcuts are used:

$$\bar{\kappa}_j := \kappa_j - i\delta\kappa_{j-1} \tag{58}$$

$$\hat{\kappa}_j := \frac{1}{\tilde{\Omega}}\kappa_{j-2} - \frac{i}{\delta}\kappa_j \tag{59}$$

$$\bar{\bar{\kappa}}_j := \frac{1}{\tilde{\Omega}}\bar{\kappa}_{j-2} - \frac{i}{\delta}\bar{\kappa}_j. \tag{60}$$

4.3 Transmission coefficient for the model chain

From the Landauer theory the transmission coefficient T is finally obtained in terms of the Green's function:

$$T = 4\delta^2 \mid g_{1,\eta} \mid^2 . \tag{61}$$

From Eq. (57) and remembering that g has been chosen so as to contain t in the wake of Eq. (17), $\mid g_{1,\eta} \mid^2$ can be evaluated to be:

To give a specific example, we have chosen the parameters $t = 3\,\mathrm{eV}, \delta = 3\,\mathrm{eV}$ and $\epsilon_\mathrm{d} = 9\,\mathrm{eV}$. The number $n = \eta - 2$ denotes the number of units inserted into the model chain except the first and the last element, which serve as coupling elements to the electrodes, as explained above. The development of T with respect to the number of chain units n is shown in Fig. 7. Significant variations with changing chain length n are observed. In particular no monotonic decline with the chain length is found. Moreover there is an obvious qualitative agreement between the model case and the curve calculated for the dithiol polyenes with orbital space 1, as can be seen from Fig. 6. In both cases there is a monotonic

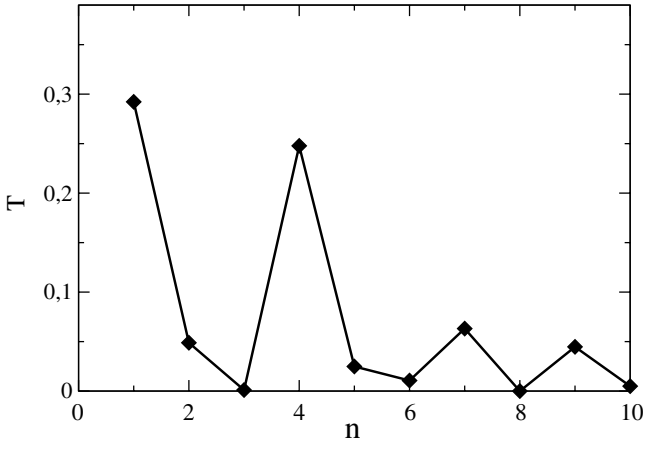

Fig. 7 Transmission coefficient T in dependence of the number n of inserted units in the model chain

decrease of T with the number of chain units n from 1 to 3, followed by an increase for the chain with four units.

The fact that this major finding of the ab initio calculations can be found in the model treatment as well can be seen as a strong reconfirmation of the former.

5 Conclusions

We have performed a systematic study of the charge transmission behavior of molecules in junctions as a function of the molecule length. In particular the transmission coefficient was computed for $S_2(CH)_{2n}$ for $n \in \{1, 2, 3, 4, 5\}$. The calculations rest on the Landauer theory and the wide band approximation. A fully ab initio wave function based procedure was mounted to obtain the Green's function entering the Landauer formula. The local incremental scheme was used with localized occupied HF orbitals throughout, whereas for the virtual space both localized and canonical HF orbitals were tested as a starting point for the sake of comparison. We found that employing the entire canonical virtual space for excitations leads to a rapid convergence of the incremental contributions to the transmission coefficient, which can be approximated to a large degree by the one–region increments alone. As a result of the series of calculations we found that while T varies with the length n of the chain, the dependence is not monotonous. In the second part an analytic formula was developed for the case of a model chain in the tight binding approximation. It turns out that the model analysis can reproduce the qualitative behavior of T as a function of the chain length to a significant extent. We conclude that such a model system might be developed further so as to give qualitative estimates for more complex systems in the future. At the same time this analytic study reconfirms our quantum chemical results for the dithiol polyenes.

Acknowledgements The authors appreciate support of the German Research Foundation DFG in the frame of the program AL 625/2–1.

References

1. Joachim C, Gimzewski JK, Aviram A (2000) Nature (London) 408:541
2. Reed MA, Zhou C, Muller CJ, Burgin TP, Tour JM (1997) Science 278:252
3. Kergueris C, Bourgoin J–P, Palacin S, Esteve D, Urbina C, Magoga M, Joachim C (1999) Phys Rev B 59:12505
4. Emberly EG, Kirczewski G (1999) Phys Rev B 60:6028
5. Di Ventra M, Pantelides ST, Lang ND (2000) App Phys Lett 76:3448
6. Di Ventra M, Pantelides ST, Lang ND (2000) Phys Rev Lett 84:979
7. Samanta MP, Tian W, Datta S et al. (1996) Phys Rev B 53:R7626
8. Lang ND, Avouris Ph (2000) Phys Rev Lett 84:358
9. Ingold G–L, Hänggi P (2002) Chem Phys 281:199
10. Rakshit T, Liang G–C, Ghosh AW, Datta S (2003) Condens Matter: 0305695 v1
11. Gutierrez R, Fagas G, Richter K, Grossmann F, Schmidt R (2003) Europhys Lett 62:90
12. Hettler MH, Wenzel W, Wegewijs MR, Schoeller H (2002) Condens Matter: 0207483 v1
13. Ghosh AW, Datta S (2003) Condens Matter: 0303630 v1
14. Todorov TN, Briggs GAD, Sutton AP (1993) J Phys: Condens Matter 5:2389
15. Paulsson M, Zahid F, Datta S (2002) Condens Matter: 0208183 v1
16. Paulsson M, Zahid F, Datta S (2006) Nanoscience, engineering and technology handbook, William Goddard (ed), CRC Press, Baca Raton (in press)
17. Mokrousov Y, Bihlmayer G, Blügel S (2005) Phys Rev B 72:045402
18. Cuniberti G, Großmann F, Gutierrez R (2002) Advances in sol state phys, vol 42, Springer
19. Cuniberti G, Fagas G, Richter K (2001) Acta Phys Pol B, 32:437
20. Heurich J, Cuevas JC, Wenzel W, Schön G (2002) Phys Rev Lett 88:256803–1
21. Xue Y, Ratner MA (2003) Phys Rev B 68:115406
22. Xue Y, Ratner MA (2003) Phys Rev B 68:115407
23. Wang B, Wang J, Guo H (1998) Phys Rev Lett 82:398
24. Taylor J, Guo H, Wang J (2001) Phys Rev B 63:245407
25. Brandbyge M, Mozos J–L, Ordejòn P, Taylor J, Stokbro K (2002) Phys Rev B 65:165401
26. Caroli C, Combescot R, Lederer D, Nozière P, Saint–James D (1971) J Phys C 4:2598
27. Cini M (1980) Phys Rev B 22:5887
28. Lang ND (1995) Phys Rev B 52:5335
29. Evers F, Weigend F, Koentropp M (2004) Phys Rev B 69:235411
30. Krstić PS, Dean DJ, Zhang XG, Keffer D, Leng YS, Cummings PT, Wells JC (2003) Comput Mater Sci 28:321
31. Delaney P, Greer JC (2004) Phys Rev Lett 93:036805
32. Ferretti A, Calzolari A, Di Felice R, Manghi F, Caldas MJ, Nardelli BM, Molinari E (2005) Phys Rev Lett 94:116802
33. Calzolari A, Marzari N, Souza I, Nardelli MB (2004) Phys Rev B 69:035108
34. Ferretti A, Calzolari A, Di Felice R, Manghi F (2005) to appear in Phys Rev B 72:1 (2005); [BZ9302] 055536PRB
35. Lee Y–S, Nardelli MB, Marzari M (2005) Phys Rev Lett 95:076804
36. Albrecht M, Igarashi J–I (2001) J Phys Soc Jap 70:1035
37. Albrecht M (2002) Theor Chem Acc 107:71
38. Albrecht M, Fulde P, Stoll H (2000) Chem Phys Lett 319:355
39. Albrecht M (2005) Theor Chem Acc 114:265
40. Albrecht M, Schnurpfeil A, Cuniberti C (2004) Phys Stat Sol b 241:2179
41. Albrecht M (2005) *Towards a frequency independent incremental ab initio scheme for the self energy*, *accepted by Theor Chem Acc*; cond–mat: 0408325
42. Yang K–H, Song B, Tian G–S, Wang Y–P, Han R–S, Han R–Q (2003) Chin Phys Lett 20:717
43. Schnurpfeil A, Song B, Albrecht M (2005) *An ab initio non–equilibrium Green's function approach to charge transport: dithiolethine*, accepted by Chin Phys Lett; Condens Matter: 0510211

44. Takahashi M, Igarashi J–I (1999) Phys Rev B 59:7373
45. Albrecht M, Fulde P (2002) Phys Stat Sol b 234:313
46. Gräfenstein J, Stoll H, Fulde P (1993) Chem Phys Lett 215:610
47. Datta S (1995) Electronic transport in mesoscopic systems, Cambridge University Press, Cambridge
48. Frisch MJ, Trucks GW, Schlegel HB, Scuseria GE, Robb MA, Cheeseman JR, Montgomery JA Jr., Vreven T, Kudin KN, Burant JC, Millam JM, Iyengar SS, Tomasi J, Barone V, Mennucci B, Cossi M, Scalmani G, Rega N, Petersson GA, Nakatsuji H, Hada M, Ehara M, Toyota K, Fukuda R, Hasegawa J, Ishida M, Nakajima T, Honda Y, Kitao O, Nakai H, Klene M, Li X, Knox JE, Hratchian HP, Cross JB, Adamo C, Jaramillo J, Gomperts R, Stratmann RE, Yazyev O, Austin AJ, Cammi R, Pomelli C, Ochterski JW, Ayala PY, Morokuma K, Voth GA, Salvador P, Dannenberg JJ, Zakrzewski VG, Dapprich S, Daniels AD, Strain MC, Farkas O, Malick K, Rabuck AD, Raghavachari K, Foresman JB, Ortiz JV, Cui Q, Baboul AG, Clifford S, Cioslowski J, Stefanov BB, Liu G, Liashenko A, Piskorz P, Komaromi I, Martin RL, Fox DJ, Keith T, Al-Laham MA, Peng CY, Nanayakkara A, Challacombe M, Gill PMW, Johnson B, Chen W, Wong MW, Gonzalez C, Pople JA (2004) Gaussian 03, Revision C.02. Gaussian Inc., Wallingford CT
49. Pipek J, Mezey PG (1989) J Chem Phys 90:4916
50. MOLPRO, a package of ab initio programs designed by Werner H-J, Knowles P J, version 2002.1, Amos R D, Bernhardsson A, Berning A, Celani P, Cooper D L, Degan M J O, Dobbyn A J, Eckert F, Hampel C, Hetzer G, Knowles P J, Korona T, Lindh R, Llyod AW, McNicholas S J, Manby F R, Meyer W, Mura M E, Nicklass A, Palmieri P, Pitzer R M, Rauhut G, Schb́futz M, Schumann U, Stoll H, Stone A J, Tarroni R, Thorsteinsson T, Werner H-J